

Effective Use of Variational Embedding Capacity in Expressive End-to-End Speech Synthesis

Eric Battenberg*, Soroosh Mariooryad, Daisy Stanton, RJ Skerry-Ryan, Matt Shannon,
David Kao, and Tom Bagby

Google Research

Abstract

Recent work has explored sequence-to-sequence latent variable models for expressive speech synthesis (supporting control and transfer of prosody and style), but has not presented a coherent framework for understanding the trade-offs between the competing methods. In this paper, we propose embedding capacity as a unified method of analyzing the behavior of latent variable models of speech, comparing existing heuristic (non-variational) methods to variational methods that are able to explicitly constrain capacity using an upper bound on representational mutual information. In our proposed model, we show that by adding conditional dependencies to the variational posterior such that it matches the form of the true posterior, the same model can be used for high-precision prosody transfer, text-agnostic style transfer, and generation of natural-sounding prior samples. For multi-speaker models, the proposed model is able to preserve target speaker identity during inter-speaker prosody transfer and when drawing samples from the latent prior. Lastly, we introduce a method for decomposing embedding capacity hierarchically across two sets of latents, allowing a portion of the latent variability to be specified and the remaining variability sampled from a learned prior.

1 Introduction

The synthesis of realistic human speech is a challenging problem that is important for natural human-computer interaction. End-to-end neural network-based approaches have seen significant progress in recent years [1–4], even matching human performance for short assistant-like utterances [5]. However, these neural models are sometimes viewed as less interpretable or controllable than more traditional models composed of multiple stages of processing that each operate on reified linguistic or phonetic representations.

Text-to-speech (TTS) is an underdetermined problem, meaning the same text input has an infinite number of reasonable spoken realizations. In addition to speaker and channel characteristics, important sources of variability in TTS include intonation, stress, and rhythm (collectively referred to as *prosody*). These attributes convey linguistic, semantic, and emotional meaning beyond what is present in the lexical representation (i.e., the text) [6]. Recent end-to-end TTS research has aimed to model and/or directly control the remaining variability in the output [7–13].

In [7], a Tacotron-like [1] model is augmented with a deterministic encoder that projects reference speech into a learned embedding space. This reference encoder can be used for prosody transfer (“say it like this”) between speakers and to text that is slightly modified relative to the reference text. However, the learned embeddings lack transfer generality in that they cannot be used with arbitrarily modified text and they do not fully preserve the characteristics of a target speaker’s voice when used for inter-speaker transfer. Speaker identity preservation issues are addressed to some extent in [10] by centering the learned embeddings using speaker-wise means.

*Correspondence to Eric Battenberg <ebattenberg@google.com>.

Other work targets *style* transfer and control, a text-agnostic variation on prosody transfer and control. The Global Style Token (GST) system [8] uses a modified reference encoder with a tighter bottleneck to transfer global style properties to arbitrary text and enable more human-accessible style control at the expense of lower-precision transfer. Another approach [13] to style transfer uses an adversarial objective to disentangle style from text.

In [9] and [11], a variational approach [14] is used to tackle the style task. Advantages of this approach include its ability to generate style samples via the accompanying prior and the potential for better disentangling between latent style factors [15]. These publications do not specify whether they directly optimize the variational evidence lower bound (ELBO) [14] during training or if they tune the weight on the Kullback-Leibler (KL) divergence term for the target task.

In this work, our primary contributions include the following:

1. We propose a unified approach for analyzing the characteristics of TTS latent variable models, independent of architecture, using the **capacity** of the learned embeddings.
2. We estimate embedding capacity for existing heuristic approaches, target specific capacities for our proposed model using a Lagrange multiplier-based optimization scheme, and show that capacity is correlated with perceptual reference similarity.
3. We show that modifying the variational posterior to match the form of the true posterior enables style and prosody transfer in the same model, helps preserve target speaker identity during inter-speaker transfer, and leads to natural-sounding prior samples even at high embedding capacities.
4. We introduce a method for controlling what fraction of the variation represented in an embedding is specified, allowing the remaining variation to be sampled from the model.

2 Measuring reference embedding capacity

2.1 Learning a reference embedding space

Existing heuristic (non-variational) end-to-end approaches to prosody and style transfer [7, 8, 10, 12] typically start with the teacher-forced reconstruction loss, (1), used to train Tacotron-like sequence-to-sequence models [1, 5] and simply augment the model with a deterministic reference encoder, $g_e(\mathbf{x})$, as shown in eq. (2).

$$L(\mathbf{x}, \mathbf{y}_T, \mathbf{y}_S) \equiv -\log p(\mathbf{x}|\mathbf{y}_T, \mathbf{y}_S) = \|\mathbf{f}_\theta(\mathbf{y}_T, \mathbf{y}_S) - \mathbf{x}\|_1 + K \quad (1)$$

$$L'(\mathbf{x}, \mathbf{y}_T, \mathbf{y}_S) \equiv -\log p(\mathbf{x}|\mathbf{y}_T, \mathbf{y}_S, g_e(\mathbf{x})) = \|\mathbf{f}_\theta(\mathbf{y}_T, \mathbf{y}_S, g_e(\mathbf{x})) - \mathbf{x}\|_1 + K \quad (2)$$

where \mathbf{x} is an audio spectrogram, \mathbf{y}_T is the input text, \mathbf{y}_S is the target speaker (if training a multi-speaker model), $\mathbf{f}_\theta(\cdot)$ is a deterministic function that maps the inputs to spectrogram predictions, and K is a normalization constant. Teacher-forcing implies that $\mathbf{f}_\theta(\cdot)$ is dependent on $\mathbf{x}_{<t}$ when predicting spectrogram frame \mathbf{x}_t . Because an ℓ_1 reconstruction loss is typically used, the likelihood is equivalent to a Laplace random vector that has means provided by $\mathbf{f}_\theta(\cdot)$ and fixed diagonal covariance (though in practice, the deterministic output of $\mathbf{f}_\theta(\cdot)$ serves as the output). Transfer is accomplished by pairing the embedding computed by the reference encoder with different text or speakers during synthesis.

In these heuristic models, the architecture of the reference encoder determines the transfer characteristics of the model. For example, in [7], prosody transfer precision is controlled by the embedding dimensionality and choice of non-linearity (tanh vs. softmax), and in [8] a particular attention-based architectural bottleneck is used. These decisions affect the information capacity of the embedding and allow the models to target a specific trade-off between transfer *precision* (how closely the output resembles the reference) and *generality* (how well an embedding works when paired with arbitrary text). Higher capacity embeddings prioritize precision and are better suited for same or similar-text prosody transfer, while lower capacity embeddings prioritize generality and are better suited for text-agnostic style transfer.

The variational extensions in [9, 11] augment the reconstruction loss in eq. (2) with a KL divergence term. This encourages a stochastic reference encoder (variational posterior), $q(\mathbf{z}|\mathbf{x})$, to align well with a prior, $p(\mathbf{z})$ (eq. (3)).

The overall loss is then equivalent to the negative ELBO of the marginal likelihood of the data [14].

$$L_{\text{ELBO}}(\mathbf{x}, \mathbf{y}_T, \mathbf{y}_S) \equiv E_{\mathbf{z} \sim q(\mathbf{z}|\mathbf{x})} [-\log p(\mathbf{x}|\mathbf{z}, \mathbf{y}_T, \mathbf{y}_S)] + D_{\text{KL}}(q(\mathbf{z}|\mathbf{x}) \| p(\mathbf{z})) \quad (3)$$

$$-\log p(\mathbf{x}|\mathbf{y}_T, \mathbf{y}_S) \leq L_{\text{ELBO}}(\mathbf{x}, \mathbf{y}_T, \mathbf{y}_S) \quad (4)$$

Controlling embedding capacity in variational models can be accomplished more directly by manipulating the KL term in (3). Recent work has shown that the KL term provides an upper bound on the mutual information between the data, \mathbf{x} , and the latent embedding, $\mathbf{z} \sim q(\mathbf{z}|\mathbf{x})$ [16–18].

$$R^{\text{AVG}} \equiv E_{\mathbf{x} \sim p_D(\mathbf{x})} [D_{\text{KL}}(q(\mathbf{z}|\mathbf{x}) \| p(\mathbf{z}))], \quad R \equiv D_{\text{KL}}(q(\mathbf{z}|\mathbf{x}) \| p(\mathbf{z})) \quad (5)$$

$$I_q(\mathbf{X}; \mathbf{Z}) \equiv E_{\mathbf{x} \sim p_D(\mathbf{x})} [D_{\text{KL}}(q(\mathbf{z}|\mathbf{x}) \| q(\mathbf{z}))], \quad q(\mathbf{z}) \equiv E_{\mathbf{x} \sim p_D(\mathbf{x})} q(\mathbf{z}|\mathbf{x}) \quad (6)$$

$$R^{\text{AVG}} = I_q(\mathbf{X}; \mathbf{Z}) + D_{\text{KL}}(q(\mathbf{z}) \| p(\mathbf{z})) \quad (7)$$

$$\implies I_q(\mathbf{X}; \mathbf{Z}) \leq R^{\text{AVG}} \quad (8)$$

where $p_D(\mathbf{x})$ is the data distribution, R is the the KL term (or *rate* [18]) in (3), R^{AVG} is the KL term averaged over the data distribution, $I_q(\mathbf{X}; \mathbf{Z})$ is the representational mutual information (the **capacity** of \mathbf{z}), and $q(\mathbf{z})$ (the *aggregated posterior* [17]) is the result of marginalizing $q(\mathbf{z}|\mathbf{x})$ over the data distribution. This brief derivation is expanded in Appendix C.1.

The bound in (8) follows from (7) and the non-negativity of the KL divergence, and (7) shows that the slack on the bound is the KL divergence between the aggregated posterior and the prior. In addition to providing a tighter bound, having a low $D_{\text{KL}}(q(\mathbf{z}) \| p(\mathbf{z}))$ is desirable when sampling from the model via the prior, because then the samples of \mathbf{z} that the decoder sees during training will be very similar to samples from the prior.

Various approaches to controlling the KL term have been proposed, including varying a weight on the KL term (β) [19] and penalizing its deviation from a target value [18, 15]. Because we would like to smoothly optimize for a specific bound on the embedding capacity, we adapt the Lagrange multiplier-based optimization approach of [20] by applying it to the KL term rather than the reconstruction term.

$$\min_{\theta} \max_{\lambda \geq 0} \{ E_{\mathbf{z} \sim q_{\theta}(\mathbf{z}|\mathbf{x})} [-\log p_{\theta}(\mathbf{x}|\mathbf{z}, \mathbf{y}_T, \mathbf{y}_S)] + \lambda (D_{\text{KL}}(q_{\theta}(\mathbf{z}|\mathbf{x}) \| p(\mathbf{z})) - C) \} \quad (9)$$

where θ are the model parameters, λ is the Lagrange multiplier, and C is the capacity limit. We constrain λ to be non-negative by passing an unconstrained parameter through a softplus non-linearity, which makes the capacity constraint a limit rather than a target. This is done to prevent the optimization procedure from attempting to increase the KL term (something that can be easily achieved by moving $q(\mathbf{z})$ away from $p(\mathbf{z})$). Here λ plays a similar role to β , but is automatically tuned by the optimization procedure to achieve the desired constraints on the KL term. We found this approach to be less tedious than tuning the KL weight by hand, and it led to more stable optimization than directly penalizing the ℓ_1 deviation from the target KL.

2.2 Estimating embedding capacity

Estimating heuristic embedding capacity Unfortunately, the heuristic methods do not come packaged with an easy way to estimate embedding capacity. We can estimate an effective capacity *ordering*, however, by measuring the test-time reconstruction loss when using the reference encoder from each method. On the left side of Figure 1, we show how the reconstruction loss varies with embedding dimensionality for the prosody transfer (tanh/softmax) and GST models described in [7] and [8] and for variational models with different KL weights, β , or different capacity limits, C . We also compare to a baseline Tacotron model without a reference encoder. For this preliminary comparison, we use the expressive single-speaker dataset and training setup described in Section 4.2.

Looking at the heuristic methods in Figure 1, we see that using a softmax non-linearity results in a more severe bottleneck than tanh, and the GST bottleneck is even more restrictive, which demonstrates how the precision/generalization trade-off is affected by changes in embedding capacity. For the variational models, using $\beta = 0.1$ matches the loss of the tanh prosody transfer model and $\beta = 10$ is similar to the GST curve. Using $\beta = 100$ yields a loss very similar to the baseline Tacotron, because the embedding capacity is effectively squashed to zero (Figure B.1 in the appendix shows how the KL term is affected).

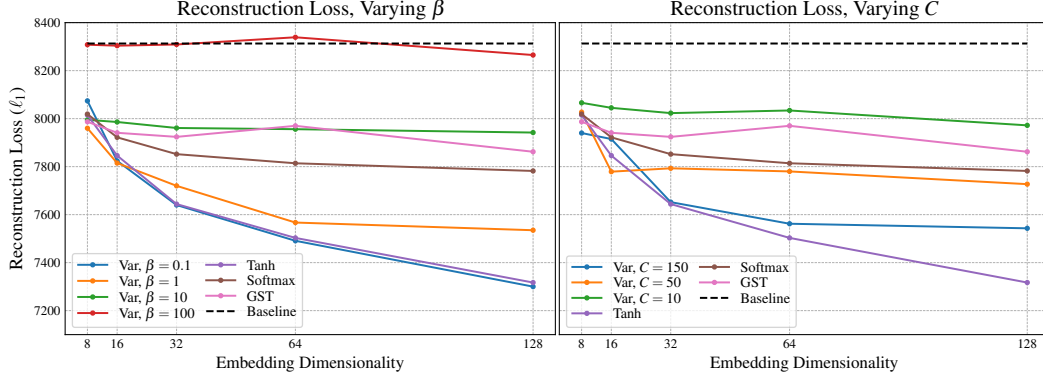


Figure 1: Reconstruction loss vs. embedding dimensionality for a variety of heuristic and variational models. [left] Controlling variational embedding capacity via the KL weight, β . [right] Controlling capacity, C , via the KL term directly. Figure B.1 in the appendix shows how the KL term is affected by β and C .

Bounding variational embedding capacity As shown on the left side of Figure 1, many factors affect effective embedding capacity, including embedding dimensionality, model architecture, and KL weight. We saw in (8) that the KL term is an upper bound on embedding capacity, so, we can directly target a specific capacity limit by constraining the KL term using the objective in eq. (9). The right side of Figure 1 shows the effect of varying the capacity limit, C .

For the three values of C in the plot, we can see that the reconstruction loss flattens out once the embedding reaches a certain dimensionality. This gives us a consistent way to control embedding capacity as it only requires using a reference encoder architecture with sufficient structural capacity (at least C) to achieve the desired representational capacity in the variational embedding. Because of this, we use 128-dimensional embeddings in all of our experiments, which should be sufficient for the range of capacities we target.

3 Making effective use of embedding capacity

3.1 Matching the form of the true posterior

In previous work [9, 11], the variational posterior has the form $q(\mathbf{z}|\mathbf{x})$, which matches the form of the true posterior for a simple generative model $p(\mathbf{x}|\mathbf{z})p(\mathbf{z})$. However, for the conditional generative model used in TTS, $p(\mathbf{x}|\mathbf{z}, \mathbf{y}_T, \mathbf{y}_S)p(\mathbf{z})$, it is missing conditional dependencies present in the true posterior, $p(\mathbf{z}|\mathbf{x}, \mathbf{y}_T, \mathbf{y}_S)$. Figure 2 shows this visually. In order to match the form of the true posterior,

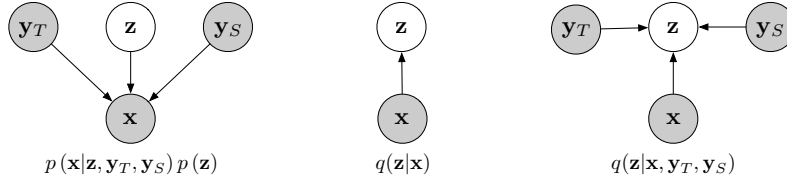


Figure 2: Adding conditional dependencies to the variational posterior. Shaded nodes indicate observed variables. [left] The true generative model. [center] Variational posterior missing conditional dependencies present in the true posterior. [right] Variational posterior that matches the form of the true posterior.

posterior, we inject information about the text and the speaker into the network that predicts the parameters of the variational posterior. Speaker information is represented as learned speaker-wise embedding vectors, while the text information is summarized into a vector by passing the output of the Tacotron text encoder through a unidirectional RNN as in [21]. Appendix A.1 gives additional details. For this work, we use a simple diagonal Gaussian for the approximate posterior, $q(\mathbf{z}|\mathbf{x}, \mathbf{y}_T, \mathbf{y}_S)$ and a standard normal distribution for the prior, $p(\mathbf{z})$. We use these distributions for simplicity and

efficiency, but more powerful distributions such as Gaussian mixtures and normalizing flows [22] could lead to better results.

Because we are learning a conditional generative model, $p(\mathbf{x}|\mathbf{y}_T, \mathbf{y}_S)$, we could have used a learned conditional prior, $p(\mathbf{z}|\mathbf{y}_T, \mathbf{y}_S)$, in order to improve the quality of the output generated when sampling via the prior. However, in this work we focus on the transfer use case where we infer $\mathbf{z}^{\text{ref}} \sim q(\mathbf{z}|\mathbf{x}^{\text{ref}}, \mathbf{y}_T^{\text{ref}}, \mathbf{y}_S^{\text{ref}})$ from a reference utterance and use it to re-synthesize speech using different text or speaker inputs, $\mathbf{x}' \sim p(\mathbf{x}|\mathbf{z}^{\text{ref}}, \mathbf{y}_T', \mathbf{y}_S')$. Using a fixed prior allows \mathbf{z} to share a high probability region across all text and speakers so that an embedding inferred from one utterance is likely to lead to non-degenerate output when being used with any other text or speaker.

3.2 Decomposing embedding capacity hierarchically

In inter-text style transfer uses cases, we infer \mathbf{z}^{ref} from a reference utterance and then use it to generate a new utterance with the same style but different text. One problem with this approach is that \mathbf{z}^{ref} completely specifies all variation that the latent embedding is capable of conveying to the decoder, $p(\mathbf{x}|\mathbf{z}^{\text{ref}}, \mathbf{y}_T, \mathbf{y}_S)$. So, even though there are many possible realizations of an utterance with a given style, this approach can produce only one².

To address this issue, we decompose the latents, \mathbf{z} , hierarchically [23] into \mathbf{z}_s and \mathbf{z}_p (the mnemonic subscripts stand for “style” and “prosody”, respectively), as shown in Figure 3. Factorizing the latents in this way allows us to specify how the joint capacity, $I_q(\mathbf{X}; [\mathbf{Z}_s, \mathbf{Z}_p])$, is divided between \mathbf{z}_s and \mathbf{z}_p .

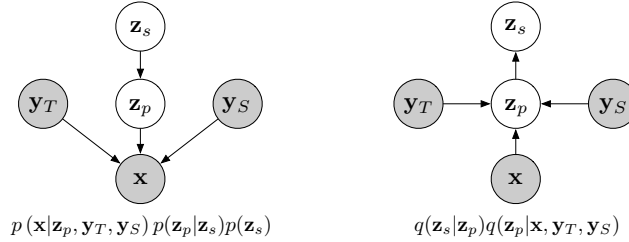


Figure 3: Hierarchical decomposition of the latents. Shaded nodes indicate observed variables. [left] The true generative model. [right] Variational posterior that matches the form of the true posterior.

As shown in eq. (8), the KL term is an upper bound on $I_q(\mathbf{X}; \mathbf{Z})$. We can also derive similar bounds for $I_q(\mathbf{X}; \mathbf{Z}_s)$ and $I_q(\mathbf{X}; \mathbf{Z}_p)$.

For $I_q(\mathbf{X}; \mathbf{Z}_p)$, we have

$$I_q(\mathbf{X}; [\mathbf{Z}_s, \mathbf{Z}_p]) \leq R^{\text{AVG}} \quad (10)$$

$$I_q(\mathbf{X}; [\mathbf{Z}_s, \mathbf{Z}_p]) = I_q(\mathbf{X}; \mathbf{Z}_p) + I_q(\mathbf{X}; \mathbf{Z}_s | \mathbf{Z}_p) = I_q(\mathbf{X}; \mathbf{Z}_p) \quad (11)$$

$$\implies I_q(\mathbf{X}; \mathbf{Z}_p) \leq R^{\text{AVG}} \quad (12)$$

where (10) was already shown in (8), and (11) follows from the chain rule for mutual information and the Markov property.

For $I_q(\mathbf{X}; \mathbf{Z}_s)$, we have

$$I_q(\mathbf{Z}_p; \mathbf{Z}_s) \leq E_{\mathbf{z}_p \sim q(\mathbf{z}_p)} [D_{KL}(q(\mathbf{z}_s | \mathbf{z}_p) \| p(\mathbf{z}_s))] \quad (13)$$

$$\equiv R_s^{\text{AVG}} \quad (14)$$

$$I_q(\mathbf{X}; \mathbf{Z}_s) \leq I_q(\mathbf{Z}_p; \mathbf{Z}_s) \quad (15)$$

$$\implies I_q(\mathbf{X}; \mathbf{Z}_s) \leq R_s^{\text{AVG}} \quad (16)$$

where (13) again follows from (8), and eq. (15) is a result of the data processing inequality. R_s makes up a portion of the overall joint KL term. Additional steps of the derivations are provided in Appendix C.2.

²If the decoder were truly stochastic, we could actually sample multiple realizations given the same \mathbf{z}^{ref} , but, at high embedding capacities the variations would likely be very similar perceptually.

Defining $R_p \equiv R - R_s$ yields the following bounds:

$$\implies I_q(\mathbf{X}; \mathbf{Z}_s) \leq R_s^{\text{AVG}}, \quad I_q(\mathbf{X}; \mathbf{Z}_p) \leq R_s^{\text{AVG}} + R_p^{\text{AVG}} \quad (17)$$

The ELBO for this model can be written as:

$$L_{\text{ELBO}}(\mathbf{x}, \mathbf{y}_T, \mathbf{y}_S) = -E_{\mathbf{z}_p \sim q(\mathbf{z}_p | \mathbf{x})} [\log p(\mathbf{x} | \mathbf{z}_p, \mathbf{y}_T, \mathbf{y}_S)] + R_s + R_p \quad (18)$$

In order to specify how the joint capacity is distributed between the latents, we extend (9) to have two Lagrange multipliers and capacity targets.

$$\min_{\theta} \max_{\lambda_s, \lambda_p \geq 0} \left\{ E_{\mathbf{z}_p \sim q_{\theta}(\mathbf{z}_p | \mathbf{x}, \mathbf{y}_T, \mathbf{y}_S)} [-\log p_{\theta}(\mathbf{x} | \mathbf{z}_p, \mathbf{y}_T, \mathbf{y}_S)] + \lambda_s(R_s - C_s) + \lambda_p(R_p - C_p) \right\} \quad (19)$$

Now we have two capacity targets: C_s limits the information capacity of \mathbf{z}_s , and C_p limits how much capacity \mathbf{z}_p has in excess of \mathbf{z}_s (i.e., the total capacity of \mathbf{z}_p is capped at $C_s + C_p$). This allows us to infer $\mathbf{z}_s^{\text{ref}} \sim q(\mathbf{z}_s | \mathbf{z}_p)q(\mathbf{z}_p | \mathbf{x}^{\text{ref}}, \mathbf{y}_T^{\text{ref}}, \mathbf{y}_S^{\text{ref}})$ from a reference utterance and use it to sample multiple realizations, $\mathbf{x}' \sim p(\mathbf{x} | \mathbf{z}_p, \mathbf{y}_T, \mathbf{y}_S)p(\mathbf{z}_p | \mathbf{z}_s^{\text{ref}})$. Intuitively, the higher C_s is, the more the output will resemble the reference, and the higher C_p is, the more variation we would expect from sample to sample when using the same $\mathbf{z}_s^{\text{ref}}$.

4 Experiments

4.1 Model architecture and training

Model architecture The baseline model we start with is a Tacotron-based [1] system that incorporates modifications from [7], including phoneme inputs instead of characters, GMM attention [24], and a WaveNet [25] neural vocoder to convert the output mel spectrograms into audio samples [5]. The decoder RNN uses a reduction factor of 2, meaning that it produces two spectrogram frames per timestep. We use the CBHG text encoder from [8] and modify the GMM attention to compute its parameters using the softplus function (rather than exp).

For the heuristic models compared in Section 2.2, we augment the baseline Tacotron with the reference encoders described in [7] and [8]. For the variational models that we compare in the following experiments, we start with the reference encoder from [7] and replace the tanh bottleneck layer with an MLP that predicts the parameters of the variational posterior. When used, the additional conditional dependencies (text and speaker) are fed into the MLP as well.

Training To train the models, the primary optimizer is run synchronously across 10 workers (2 of them backup workers) for 300,000 training steps with an effective batch size of 256. It uses the Adam algorithm [26] with a learning rate that is annealed from 10^{-3} to 5×10^{-5} over 200,000 training steps. The optimizer for the Lagrange parameter is run asynchronously on the 10 workers and uses SGD with momentum 0.9 and a fixed learning rate of 10^{-5} . Separate optimizers are necessary because attempting to combine the objectives in the primary Adam optimizer leads to very slow optimization of the Lagrange parameter.

Additional architectural and training details are provided in Appendix A.

4.2 Experiment setup

Datasets For single-speaker models, we use an expressive audiobook dataset consisting of 50,086 training utterances (36.5 hours) and 912 test utterances. Multi-speaker models are trained using data from 58 voice assistant-like speakers, consisting of 419,966 training utterances (327 hours). We evaluate on a 9-speaker subset of the multi-speaker test data, consisting of 1808 utterances.

Tasks The tasks that we explore include same-text prosody transfer, inter-text style transfer, and inter-speaker prosody transfer. We also evaluate the quality of samples produced via the prior. For these tasks, we compare performance when using variational models with and without the additional conditional dependencies in the variational posterior at a number of different capacity limits. For models with hierarchical latents, we demonstrate the effect of varying C_s and C_p for same-text prosody transfer when inferring \mathbf{z}_s and sampling \mathbf{z}_p or when inferring \mathbf{z}_p directly.

Evaluation We use crowd-sourced native speakers to collect two types of subjective evaluations. First, mean opinion score (MOS) rates naturalness on a scale of 1-5, 5 being the best. Second, we

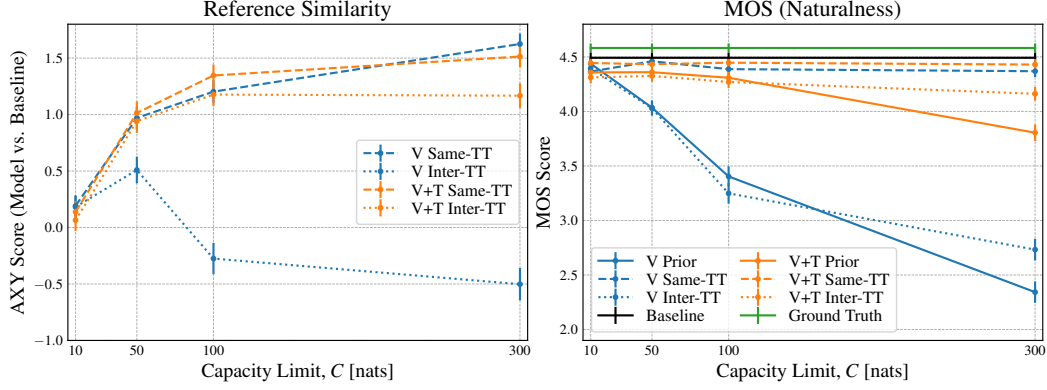


Figure 4: Comparing same-text transfer, inter-text transfer, and prior samples for variational models with and without text dependencies in the variational posterior (V+T and V, respectively). Error bars show 95% confidence intervals for the subjective evaluations.

use the AXY side-by-side comparison proposed in [7] to measure subjective similarity to a reference utterance relative to the baseline model on a scale of $[-3, 3]$. We also use an objective similarity metric that uses dynamic time warping to find the minimum mel cepstral distortion [27] between two sequences (MCD-DTW). Lastly, for inter-speaker transfer, we follow [7] and use a simple speaker classifier to measure how well speaker identity is preserved. Additional details on evaluation methodologies are provided in Appendix A.

4.3 Results

Single speaker For single-speaker models, we compare the performance on same and inter-text transfer and the quality of samples generated via the prior for models with and without text conditioning in the variational posterior (V+T and V, respectively) at different capacity limits, C . Similarity results for the transfer task are shown on the left side of Figure 4 and demonstrate increasing reference similarity as C is increased, with the exception of the V model on the inter-text transfer task. Looking at the MOS naturalness results on the right side of Figure 4, we see that both inter-text transfer and prior sampling take a serious hit as capacity is increased for the V model, while the V+T model is able to maintain respectable performance even at very high capacities on all tasks. Because the posterior in the V model doesn’t have access to the text, it is likely that the model has to divide the latent space into regions that correspond to different utterance lengths, which means that an arbitrary z (sampled from the prior or inferred from a reference) is unlikely to pair well with text of an arbitrary length.

Multi-speaker For multi-speaker models, we compare inter-speaker transfer performance and prior sample quality with and without speaker conditioning in the variational posterior (V+T+S and V+T, respectively) at a fixed capacity limit of 150 nats. In Table 1, we see that both models are significantly more similar to the reference compared to the baseline model, while the V+T+S model has an edge in MOS for both inter-speaker transfer and prior samples (almost matching the MOS of the deterministic baseline model even at high embedding capacity). The speaker classifier results show that the V+T+S model preserves target speaker identity about as well as the baseline model and ground truth data ($\sim 5\%$ of the time the classifier chooses a speaker other than the target speaker), whereas for the V+T model this happens about 22% of the time. Though 22% seems like a large speaker error rate, it is much lower than the 79% figure presented in [7] for a heuristic prosody transfer model. This demonstrates that even with a weakly conditioned posterior, the capacity limiting properties of variational models lead to better transfer generality and robustness.

Hierarchical latents To evaluate hierarchical decomposition of capacity in a single speaker setting, we use the MCD-DTW distance to quantify reference similarity and inter-sample variability when conditioning on the same reference. As shown in Table B.1 in the appendix, MCD-DTW strongly (negatively) correlates with subjective similarity. The left side of Figure 5 shows results for samples generated using a z_s inferred from the reference. As C_s is increased, we see a strong downward trend in the average distance to the reference. We can also see that for a fixed C_s , increasing C_p results in a larger amount of sample-to-sample variation (average MCD-DTW between samples)

Table 1: Inter-speaker same-text transfer results for $C = 150$ with and without speaker dependencies in the variational posterior (V+T+S and V+T, respectively). SpID denotes the fraction of the time the target speaker was chosen by the speaker classifier. For reference, we provide MOS and SpID numbers for the baseline model and ground truth audio (though neither of them are “prior” samples).

Model	Inter-Speaker Transfer			Prior Samples	
	Ref. Similarity	MOS	SpID	MOS	SpID
V+T	0.364 ± 0.104	3.994 ± 0.066	80.1%	3.674 ± 0.077	78.0%
V+T+S	0.439 ± 0.087	4.099 ± 0.061	95.8%	3.906 ± 0.066	94.9%
Baseline				4.086 ± 0.060	95.7%
Ground Truth				4.535 ± 0.044	96.9%

when drawing samples using the same \mathbf{z}_s . The right side of Figure 5 shows the same metrics but for samples generated using a \mathbf{z}_p inferred from the reference. In this case, we see a slight downward trend in the reference distance as the total capacity limit, C , is increased (the trend is less dramatic because the capacity is already fairly high). We also see significantly lower inter-sample distance because the variation modeled by the latents is completely specified by \mathbf{z}_p (in this case, we sample multiple \mathbf{z}_p ’s from $q(\mathbf{z}_p|\mathbf{x}^{\text{ref}}, \mathbf{y}_T)$ because using the same \mathbf{z}_p would lead to identical output from the deterministic decoder).

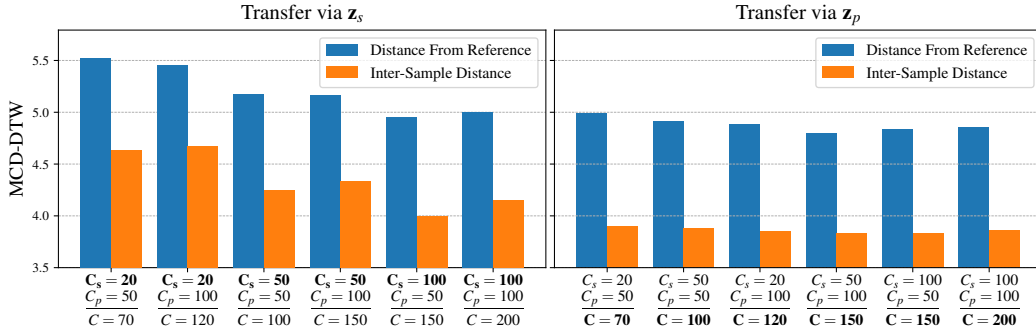


Figure 5: MCD-DTW reference distance and inter-sample distance for hierarchical latents when transferring via \mathbf{z}_s and \mathbf{z}_p .

To appreciate the results fully, it is strongly recommend to listen to the audio examples available on the web³ or in the supplementary materials.

5 Conclusion

We have proposed embedding capacity (which correlates with reference similarity for transfer use cases and variability for sampling use cases) as a useful framework for comparing latent variable models of speech. Our proposed model shows that including text and speaker dependencies in the variational posterior is crucial for a variety of transfer and sampling tasks. Motivated by the multi-faceted variability of natural human speech, we also showed that embedding capacity can be decomposed hierarchically in order to control a trade-off between transfer fidelity and sample variation.

There are many directions for future work, including adapting the fixed-length variational embeddings to be variable-length and synchronous with either the text or audio, using more powerful distributions like normalizing flows, and replacing the deterministic decoder outputs with a proper likelihood distribution. For transfer and control uses cases, the ability to distribute certain speech characteristics across subsets of the hierarchical latents would allow more fine-grained control of different aspects of the output speech. For purely generative, non-transfer use cases, using more powerful conditional priors could improve sample quality.

³<https://google.github.io/tacotron/publications/capacitron>

References

- [1] Yuxuan Wang, RJ Skerry-Ryan, Daisy Stanton, Yonghui Wu, Ron J. Weiss, Navdeep Jaitly, Zongheng Yang, Ying Xiao, Zhifeng Chen, Samy Bengio, Quoc Le, Yannis Agiomyrgiannakis, Rob Clark, and Rif A. Saurous. Tacotron: Towards end-to-end speech synthesis. In *Proceedings of Interspeech*, August 2017.
- [2] Yaniv Taigman, Lior Wolf, Adam Polyak, and Eliya Nachmani. Voiceloop: Voice fitting and synthesis via a phonological loop. In *International Conference on Learning Representations*, 2018.
- [3] Wei Ping, Kainan Peng, Andrew Gibiansky, Sercan O. Arik, Ajay Kannan, Sharan Narang, Jonathan Raiman, and John Miller. Deep voice 3: 2000-speaker neural text-to-speech. In *International Conference on Learning Representations*, 2018.
- [4] Jose Sotelo, Soroush Mehri, Kundan Kumar, Joao Felipe Santos, Kyle Kastner, Aaron Courville, and Yoshua Bengio. Char2wav: End-to-end speech synthesis. In *International Conference on Learning Representations, Workshop Track*, 2017.
- [5] Jonathan Shen, Ruoming Pang, Ron J Weiss, Mike Schuster, Navdeep Jaitly, Zongheng Yang, Zhifeng Chen, Yu Zhang, Yuxuan Wang, Rj Skerrv-Ryan, et al. Natural tts synthesis by conditioning wavenet on mel spectrogram predictions. In *2018 IEEE International Conference on Acoustics, Speech and Signal Processing (ICASSP)*, 2018.
- [6] Michael Wagner and Duane G Watson. Experimental and theoretical advances in prosody: A review. *Language and cognitive processes*, 25(7-9):905–945, 2010.
- [7] RJ Skerry-Ryan, Eric Battenberg, Ying Xiao, Yuxuan Wang, Daisy Stanton, Joel Shor, Ron Weiss, Rob Clark, and Rif A. Saurous. Towards end-to-end prosody transfer for expressive speech synthesis with Tacotron. In *Proceedings of the 35th International Conference on Machine Learning*, 2018.
- [8] Yuxuan Wang, Daisy Stanton, Yu Zhang, RJ-Skerry Ryan, Eric Battenberg, Joel Shor, Ying Xiao, Ye Jia, Fei Ren, and Rif A Saurous. Style tokens: Unsupervised style modeling, control and transfer in end-to-end speech synthesis. In *International Conference on Machine Learning*, pages 5167–5176, 2018.
- [9] Wei-Ning Hsu, Yu Zhang, Ron Weiss, Heiga Zen, Yonghui Wu, Yuan Cao, and Yuxuan Wang. Hierarchical generative modeling for controllable speech synthesis. In *International Conference on Learning Representations*, 2019.
- [10] Younggun Lee and Taesu Kim. Robust and fine-grained prosody control of end-to-end speech synthesis. In *ICASSP 2019-2019 IEEE International Conference on Acoustics, Speech and Signal Processing (ICASSP)*, pages 5911–5915. IEEE, 2019.
- [11] Ya-Jie Zhang, Shifeng Pan, Lei He, and Zhen-Hua Ling. Learning latent representations for style control and transfer in end-to-end speech synthesis. In *ICASSP 2019-2019 IEEE International Conference on Acoustics, Speech and Signal Processing (ICASSP)*, pages 6945–6949. IEEE, 2019.
- [12] Gustav Eje Henter, Xin Wang, and Junichi Yamagishi. Deep encoder-decoder models for unsupervised learning of controllable speech synthesis. *arXiv preprint arXiv:1807.11470*, 2018.
- [13] Shuang Ma, Daniel Mcduff, and Yale Song. A generative adversarial network for style modeling in a text-to-speech system. In *International Conference on Learning Representations*, 2019.
- [14] Diederik P Kingma and Max Welling. Auto-Encoding Variational Bayes. In *International Conference on Learning Representations*, 2014.
- [15] Christopher P Burgess, Irina Higgins, Arka Pal, Loic Matthey, Nick Watters, Guillaume Desjardins, and Alexander Lerchner. Understanding disentangling in β -vae. *arXiv preprint arXiv:1804.03599*, 2018.

- [16] Matthew D Hoffman and Matthew J Johnson. Elbo surgery: yet another way to carve up the variational evidence lower bound. In *Workshop in Advances in Approximate Bayesian Inference, NIPS*, 2016.
- [17] Alireza Makhzani, Jonathon Shlens, Navdeep Jaitly, and Ian Goodfellow. Adversarial autoencoders. In *International Conference on Learning Representations*, 2016.
- [18] Alexander Alemi, Ben Poole, Ian Fischer, Joshua Dillon, Rif A Saurous, and Kevin Murphy. Fixing a broken elbo. In *International Conference on Machine Learning*, pages 159–168, 2018.
- [19] Irina Higgins, Loic Matthey, Arka Pal, Christopher Burgess, Xavier Glorot, Matthew Botvinick, Shakir Mohamed, and Alexander Lerchner. beta-vae: Learning basic visual concepts with a constrained variational framework. In *International Conference on Learning Representations*, 2017.
- [20] Danilo Jimenez Rezende and Fabio Viola. Taming VAEs. *arXiv preprint arXiv:1810.00597*, 2018.
- [21] Daisy Stanton, Yuxuan Wang, and RJ Skerry-Ryan. Predicting expressive speaking style from text in end-to-end speech synthesis. In *2018 IEEE Spoken Language Technology Workshop (SLT)*, pages 595–602. IEEE, 2018.
- [22] Danilo Rezende and Shakir Mohamed. Variational inference with normalizing flows. In *International Conference on Machine Learning*, pages 1530–1538, 2015.
- [23] Casper Kaae Sønderby, Tapani Raiko, Lars Maaløe, Søren Kaae Sønderby, and Ole Winther. Ladder variational autoencoders. In *Advances in neural information processing systems*, pages 3738–3746, 2016.
- [24] Alex Graves. Generating sequences with recurrent neural networks. *arXiv preprint arXiv:1308.0850*, 2013.
- [25] Aäron van den Oord, Sander Dieleman, Heiga Zen, Karen Simonyan, Oriol Vinyals, Alex Graves, Nal Kalchbrenner, Andrew Senior, and Koray Kavukcuoglu. Wavenet: A generative model for raw audio. In *9th ISCA Speech Synthesis Workshop*, 2016.
- [26] Diederik Kingma and Jimmy Ba. Adam: A method for stochastic optimization. *International Conference for Learning Representations*, 2015.
- [27] R Kubichek. Mel-cepstral distance measure for objective speech quality assessment. In *Communications, Computers and Signal Processing, 1993., IEEE Pacific Rim Conference on*, volume 1, pages 125–128. IEEE, 1993.
- [28] Meinard Müller. Dynamic time warping. *Information retrieval for music and motion*, pages 69–84, 2007.

Appendix

A Experiment details

A.1 Architecture details

Baseline Tacotron The baseline Tacotron we start with (which serves as $f_{\theta}(\cdot)$ in eq. (1)) is similar to the original sequence-to-sequence model described in [1] but uses some modifications introduced in [7]. Input to the model consists of sequences of phonemes produced by a text normalization pipeline rather than character inputs. The CBHG text encoder from [1] is used to convert the input phonemes into a sequence of text embeddings. Before being fed to the CBHG encoder, the phoneme inputs are converted to learned 256-dimensional embeddings and passed through a pre-net composed of two fully connected ReLU layers (with 256 and 128 units, respectively), with dropout of 0.5 applied to the output of each layer. For multi-speaker models, a learned embedding for the target speaker is broadcast-concatenated to the output of the text encoder.

The attention module uses a single LSTM layer with 256 units and zoneout of 0.1 followed by an MLP with 128 tanh hidden units to compute parameters for the monotonic 5-component GMM attention window. Instead of using the exponential function to compute the shift and scale parameters of the GMM components as in [24], we use the softplus function, which we found leads to faster alignment and more stable optimization.

The autoregressive decoder module consists of 2 LSTM layers each with 256 units, zoneout of 0.1, and residual connections between the layers. The spectrogram output is produced using a linear layer on top of the 2 LSTM layers, and we use a reduction factor of 2, meaning we predict two spectrogram frames for each decoder step. The decoder is fed the last frame of its most recent prediction (or the previous ground truth frame during training) and the current context as computed by the attention module. Before being fed to the decoder, the previous prediction is passed through the same pre-net used before the text encoder above.

Mel spectrograms The mel spectrograms the model predicts are computed from 24kHz audio using a frame size of 50ms, a hop size of 12.5ms, an FFT size of 2048, and a Hann window. From the FFT energies, we compute 80 mel bins distributed between 80Hz and 12kHz.

Reference encoder The common reference encoder we use to compute reference embeddings starts with the mel spectrogram from the reference and passes it through a stack of 6 convolutional layers, each using ReLU non-linearities, 3x3 filters, 2x2 stride, and batch normalization. The 6 layers have 32, 32, 64, 64, 128, and 128 filters, respectively. The output of this convolution stack is fed into a unidirectional LSTM with 128 units, and the final output of the LSTM serves as the output of our basic reference encoder.

To replicate the prosody transfer model from [7], we pass the reference encoder output through an additional tanh or softmax bottleneck layer to compute the embedding. For the Style Tokens model in [8], we pass the output through the Style Tokens bottleneck described in the paper. For the approximate posterior in our variational models, we pass the output of the reference encoder (and potentially vectors describing the text and/or speaker) through an MLP with 128 tanh hidden units to produce the parameters of the diagonal Gaussian posterior which we sample from to produce a reference embedding. For all models with reference encoders, the resulting reference embedding is broadcast-concatenated to the output of the text encoder.

Conditional inputs When providing information about the text to the variational posterior, we pass the sequence of text embeddings produced by the text encoder to a unidirectional RNN with 128 units and use its final output as a fixed-length text summary that is passed to the posterior MLP. Speaker information is passed to the posterior MLP via a learned speaker embedding.

A.2 Training Details

For the optimization problems shown in eqs. (9) and (19), we use two separate optimizers. The first minimizes the objective with respect to the model parameters using the SyncReplicasOptimizer⁴ from Tensorflow with 10 workers (2 of them backup workers) and an effective batch size of 256. This

⁴https://www.tensorflow.org/api_docs/python/tf/train/SyncReplicasOptimizer

optimizer uses the Adam algorithm [26] with $\beta_1 = 0.9$, $\beta_2 = 0.999$, $\epsilon = 10^{-8}$, and a learning rate that is set to 10^{-3} , 5×10^{-4} , 3×10^{-4} , 10^{-4} , and 5×10^{-5} at 50k, 100k, 150k, and 200k steps, respectively. Training is run for 300k steps total.

The optimizer that maximizes the objective with respect to the Lagrange multiplier is run asynchronously across the 10 workers (meaning each worker computes an independent update using its 32-example sub-batch) and uses SGD with a momentum of 0.9 and a learning rate of 10^{-5} . The Lagrange multiplier is computed by passing an unconstrained parameter through the softplus function in order to enforce non-negativity. The initial value of the parameter is chosen such that the Lagrange multiplier equals 1 at the start of training.

A.3 Evaluation Details

Subjective evaluation Details for the subjective reference similarity and MOS naturalness evaluations are provided in Figures A.1 and A.2. To evaluate reference similarity, we use the AXY side-by-side template in Figure A.1, where A is the reference utterance, and X and Y are outputs from the model being tested and the baseline model.

Instructions	<p>IMPORTANT: This task requires you listen to audio samples using headphones in a quiet environment. Please release this task if:</p> <ol style="list-style-type: none"> 1. you do not have headphones, or 2. there is background noise, or 3. you think you do not have good listening ability, or 4. for any reason, you can't hear the audio samples 	
	<p>For this task, you will be given a reference speech and will be asked to decide which of two speech samples more closely matches its prosody (i.e. intonation, stress and flow).</p>	
	<p>You will first be presented with audio of a reference speech sample. First listen to the audio for the reference. Next, listen to two different speech samples and decide which sounds "closer" to the reference speech sample in terms of its prosody.</p>	
	<p>The text spoken and the speaker will be the same for both speech samples, but may differ from that of the reference speech sample.</p> <p>After listening to the left speech, please wait at least 2 seconds before listening to the right speech. Feel free to re-listen to the reference sample before listening to the right speech.</p> <p>Please ignore pronunciation issues and audio quality differences. Please focus only on the prosody, which could be indicated by differences in any of the following:</p> <ul style="list-style-type: none"> • The pitch, and how it rises or falls throughout the speech sample. • Stress put on each word or syllable (e.g. loudness or pitch changes). • Speaking rate, and how it changes throughout the speech sample. • Pause lengths. <p>Please give your qualitative opinion. If one sample feels closer but you cannot articulate why, that is OK.</p>	
How are you listening to these speech samples?	<p><input type="radio"/> Headphones, with no noise in the background. I am listening to the speech samples using headphones and there is no noise around me (people talking, music playing, air-conditioners, and fans, etc.).</p> <p><input type="radio"/> Headphones, with some low-level noise in the background. I am listening to the speech samples using headphones and there is some low-level noise around me (people talking, music playing, air-conditioners, and fans, etc.).</p> <p><input type="radio"/> Audio speakers or other (Please release the task).</p>	
The reference for the speech sample you are rating	I don't know at all.	
The audio for the reference	<div>Play Reference Speech</div>	
Text of the speech samples	I don't know at all.	
speech samples you will listen to	<div>Play Left Speech</div>	<div>Play Right Speech</div>
Are there any problems with the sample? (check only if applicable)	<input type="checkbox"/> There is a problem with the left speech sample (please comment)	<input type="checkbox"/> There is a problem with the right speech sample (please comment)
Which side sounds closer to the reference?	<div> <div>much closer</div> <div>closer</div> <div>slightly closer</div> <div>about the same</div> <div>slightly closer</div> <div>closer</div> <div>much closer</div> </div>	
What makes your preferred side closer?	<div></div>	

Figure A.1: Evaluation template for AXY prosodic reference similarity side-by-side evaluations. A human rater is presented with three stimuli: a reference speech sample (A), and two competing samples (X and Y) to evaluate. The rater is asked to rate whether the prosody of X or Y is closer to that of the reference on a 7-point scale. The scale ranges from "X is much closer" to "Both are about the same distance" to "Y is much closer", and can naturally be mapped on the integers from -3 to 3. Prior to collecting any ratings, we provide the raters with 4 examples of prosodic attributes to evaluate (intonation, stress, speaking rate, and pauses), and explicitly instruct the raters to ignore audio quality or pronunciation differences. For each triplet (A, X, Y) evaluated, we collect 1 rating, and no rater is used for more than 6 items in a single evaluation. To analyze the data from these subjective tests, we average the scores and compute 95% confidence intervals.

Instruction

IMPORTANT:
 In this project, you will listen to audio samples. Please release this task if any of the following is true:
 1) You do not have headphones
 2) You think you do not have good listening ability
 3) There is considerable background noise (street noise, loud fan/air-conditioner, open TV/radio, people talking, etc).
 4) For any reason, you can't hear the audio samples

AUDIO DEVICE (Headphones):
 1) There are many types of headphones. If you have more than one type, this is the preferred order: (a) closed-back headphones, (b) open-back headphones, (c) any other type of headphones.
 If you are not sure which type you have, please see this [Wikipedia article](#).
 2) Please set the volume of your audio device to a comfortable level.

In this task, we would like you to listen to a speech sentence and then choose a score for the audio sample you've just heard. This score should reflect your opinion of how **natural** or **unnatural** the sentence sounded. You should not judge the grammar or the content of the sentence, just how it **sounds**.
 Please:
 1) Listen to each sample at least **twice**, with at least a **one sec break** between them.
 2) Use the given 5-point scale to rate the naturalness of the speech sample. The following table provides a description of each **naturalness** level of the scale, as well as one or more reference speech example(s) for each level. Review the table and listen to all of the references. **Important note: you do not need to listen to the references if you have listened to them before.**

In-Between Ratings: Please note that you are allowed to assign "in-between" ratings (for example, a rating between "Excellent and Good"). Feel free to use them if you think the quality of the speech sample falls between two levels.

Naturalness Scale:

Score	Naturalness	Description	Reference
5.0	Excellent	Completely natural speech	Listen
4.0	Good	Mostly natural speech	Listen
3.0	Fair	Equally natural and unnatural speech	Listen
2.0	Poor	Mostly unnatural speech	Listen
1.0	Bad	Completely unnatural speech	Listen

How are you listening to the speech sample?

☐ **Headphones, with no noise in the background.** I am listening to the speech sample using headphones and there is **no** noise around me (people talking, music playing, air-conditioners, and fans, etc.).
☐ **Headphones, with some low-level noise in the background.** I am listening to the speech sample using headphones and there is some **low-level** noise around me (people talking, music playing, air-conditioners, and fans, etc.).
☐ **Audio speakers or other.**

Speech sample (please listen at least twice)

▶ 0:00 / 0:02 🔊 ⋮

Please rate the naturalness of the speech sample:

Score	Naturalness	Description
<input type="radio"/> 5.0	Excellent	Completely natural speech
<input type="radio"/> 4.5		
<input type="radio"/> 4.0	Good	Mostly natural speech
<input type="radio"/> 3.5		
<input type="radio"/> 3.0	Fair	Equally natural and unnatural speech
<input type="radio"/> 2.5		
<input type="radio"/> 2.0	Poor	Mostly unnatural speech
<input type="radio"/> 1.5		
<input type="radio"/> 1.0	Bad	Completely unnatural speech

Comments

Figure A.2: Evaluation template for mean opinion score (MOS) naturalness ratings. A human rater is presented with a single speech sample and is asked to rate perceived naturalness on a scale of 1–5, where 1 is “Bad” and 5 is “Excellent”. For each sample, we collect 1 rating, and no rater is used for more than 6 items in a single evaluation. To analyze the data from these subjective tests, we average the scores and compute 95% confidence intervals. Natural human speech is typically rated around 4.5.

MCD-DTW We evaluate the models with hierarchical latents using the MCD-DTW distance to quantify reference similarity and the amount of inter-sample variation. To compute mel cepstral distortion (MCD) [27], we use the same mel spectrogram parameters described in A.1 and take the DCT to compute the first 13 MFCCs (not including the 0th coefficient). The MCD between two frames is the Euclidean distance between their MFCC vectors. Then we use the dynamic time warping (DTW) algorithm [28] (with a warp penalty of 1.0) to find an alignment between two spectrograms that produces the minimum MCD cost (including the total warp penalty). We report the average per-frame MCD-DTW.

To evaluate reference similarity, we simply compute the MCD-DTW between the synthesized audio and the reference audio (a lower MCD-DTW indicates higher similarity). The strong (negative) correlation between MCD-DTW and subjective similarity is demonstrated in Table B.1. To quantify inter-sample variation, we compute 5 output samples using the same reference and compute the average MCD-DTW between the first sample and each subsequent sample.

B Additional results

Rate-distortion plots In Figure B.1, we augment the reconstruction loss plots from Figure 1 with additional rate/distortion plots [18].

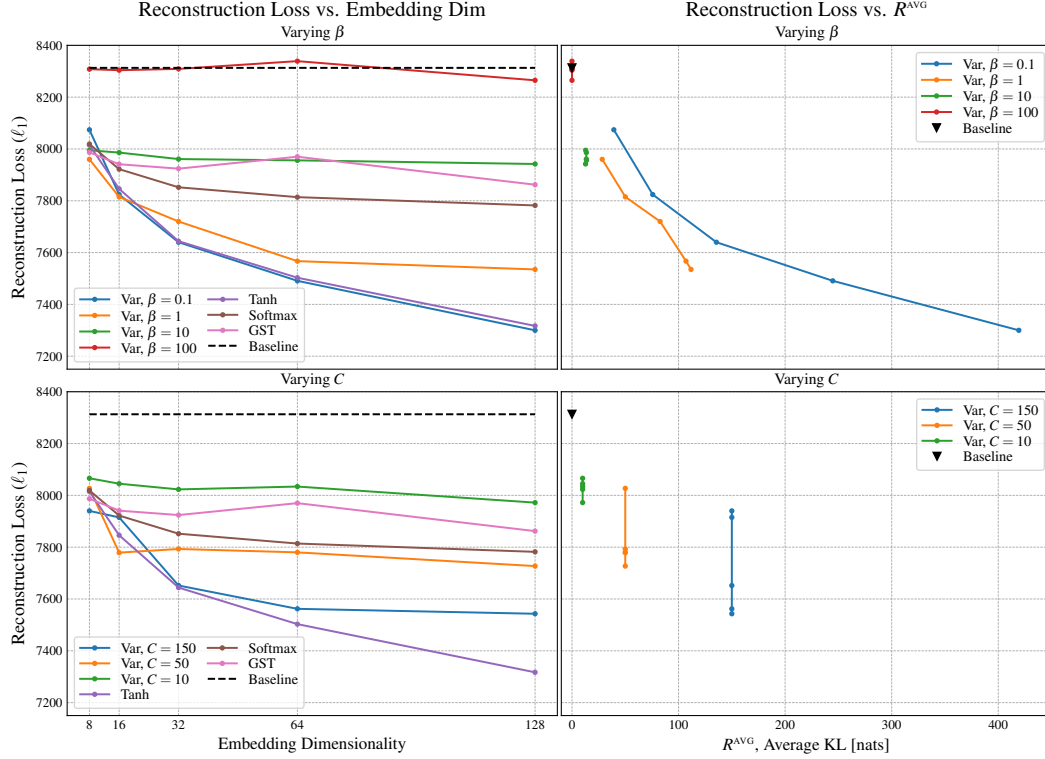


Figure B.1: Figure 1 with additional plots showing reconstruction loss vs. the average KL term. In these plots we can see how R^{avg} varies with embedding dimensionality for constant KL weight, β , while using the KL constraint from the optimization problem in eq. 9 achieves constant R^{avg} .

Single-speaker similarity and naturalness results Tables B.1 and B.2 list the raw numbers used in the single-speaker reference similarity and MOS naturalness plots shown in Figure 4 in the main paper. Also shown is MCD-DTW reference distance alongside subjective reference similarity.

Table B.1: Detailed subjective reference similarity scores and objective MCD-DTW reference distance for single speaker models at different capacity limits, C , and with and without text conditioning in the variational posterior (V+T and V, respectively). Notice how subjective reference similarity for same-text transfer is strongly negatively correlated with MCD-DTW.

Model	Ref. Similarity		MCD-DTW
	Same-TT	Inter-TT	Same-TT
V($C=10$)	0.192 ± 0.093	0.182 ± 0.097	5.67
V($C=50$)	0.970 ± 0.102	0.509 ± 0.118	5.13
V($C=100$)	1.203 ± 0.102	-0.275 ± 0.139	5.04
V($C=300$)	1.625 ± 0.092	-0.502 ± 0.143	4.81
V+T($C=10$)	0.138 ± 0.097	0.065 ± 0.095	5.68
V+T($C=50$)	1.014 ± 0.102	0.942 ± 0.104	5.11
V+T($C=100$)	1.346 ± 0.096	1.177 ± 0.103	4.94
V+T($C=300$)	1.514 ± 0.095	1.167 ± 0.110	4.83

Hierarchical latents results The similarity and inter-sample variability results for hierarchical latents from Figure 5 are shown in table format in Table B.3.

Table B.2: MOS naturalness scores for single speaker models at different capacity limits, C , with and without text conditioning in the variational posterior (V+T and V, respectively). Scores are shown for prior samples (Prior), same-text transfer (Same-TT), and inter-text transfer (Inter-TT). These results are visualized in Figure 4 in the main paper.

Model	MOS score		
	Prior	Same-TT	Inter-TT
Ground Truth	4.582 \pm 0.041		
Base	4.492 \pm 0.048		
V($C=10$)	4.438 \pm 0.049	4.366 \pm 0.053	4.396 \pm 0.049
V($C=50$)	4.035 \pm 0.066	4.460 \pm 0.051	4.029 \pm 0.067
V($C=100$)	3.404 \pm 0.093	4.388 \pm 0.055	3.249 \pm 0.095
V($C=300$)	2.343 \pm 0.098	4.369 \pm 0.054	2.733 \pm 0.099
V+T($C=10$)	4.358 \pm 0.056	4.444 \pm 0.052	4.312 \pm 0.053
V+T($C=50$)	4.360 \pm 0.053	4.433 \pm 0.052	4.326 \pm 0.054
V+T($C=100$)	4.309 \pm 0.056	4.447 \pm 0.048	4.270 \pm 0.055
V+T($C=300$)	3.805 \pm 0.076	4.430 \pm 0.050	4.162 \pm 0.062

Table B.3: Transfer using hierarchical latents. “Ref.” is the the average MCD-DTW distance from the reference, and “X-samp.” is the average inter-sample MCD-DTW. These are the numbers used in the plots in Figure 5.

(a) Transfer via \mathbf{z}_s .					(b) Transfer via \mathbf{z}_p .				
Capacity Limits			MCD-DTW		Capacity Limits			MCD-DTW	
\mathbf{C}_s	C_p	C	Ref.	X-samp.	C_s	C_p	\mathbf{C}	Ref.	X-samp.
0	0	0	6.054	-	0	0	0	6.054	-
20	50	70	5.517	4.638	20	50	70	4.991	3.899
20	100	120	5.453	4.670	50	50	100	4.916	3.876
50	50	100	5.172	4.245	20	100	120	4.882	3.847
50	100	150	5.166	4.332	100	50	150	4.834	3.830
100	50	150	4.952	3.999	50	100	150	4.797	3.832
100	100	200	5.000	4.147	100	100	200	4.852	3.858

C Derivations

C.1 Bounding representational mutual information

Definitions:

$$R \equiv \int q(\mathbf{z}|\mathbf{x}) \log \frac{q(\mathbf{z}|\mathbf{x})}{p(\mathbf{z})} d\mathbf{z} \quad (\text{KL term}) \quad (20)$$

$$R^{\text{AVG}} \equiv \iint p_D(\mathbf{x}) q(\mathbf{z}|\mathbf{x}) \log \frac{q(\mathbf{z}|\mathbf{x})}{p(\mathbf{z})} d\mathbf{x} d\mathbf{z} \quad (\text{Average KL term}) \quad (21)$$

$$I_q(\mathbf{X}; \mathbf{Z}) \equiv \iint p_D(\mathbf{x}) q(\mathbf{z}|\mathbf{x}) \log \frac{q(\mathbf{z}|\mathbf{x})}{q(\mathbf{z})} d\mathbf{x} d\mathbf{z} \quad (\text{Representational mutual information}) \quad (22)$$

$$q(\mathbf{z}) \equiv \int p_D(\mathbf{x}) q(\mathbf{z}|\mathbf{x}) d\mathbf{x} \quad (\text{Aggregated posterior}) \quad (23)$$

KL non-negativity:

$$\int q(x) \log \frac{q(x)}{p(x)} dx \geq 0 \quad (24)$$

$$\implies \int q(x) \log q(x) \geq \int q(x) \log p(x) dx \quad (25)$$

Mutual information is upper bounded by the average KL [18]:

$$I_q(\mathbf{X}; \mathbf{Z}) \equiv \iint p_D(\mathbf{x}) q(\mathbf{z}|\mathbf{x}) \log \frac{q(\mathbf{z}|\mathbf{x})}{q(\mathbf{z})} d\mathbf{x} d\mathbf{z} \quad (26)$$

$$= \iint p_D(\mathbf{x}) q(\mathbf{z}|\mathbf{x}) \log q(\mathbf{z}|\mathbf{x}) d\mathbf{x} d\mathbf{z} - \iint p_D(\mathbf{x}) q(\mathbf{z}|\mathbf{x}) \log q(\mathbf{z}) d\mathbf{x} d\mathbf{z} \quad (27)$$

$$= \iint p_D(\mathbf{x}) q(\mathbf{z}|\mathbf{x}) \log q(\mathbf{z}|\mathbf{x}) d\mathbf{x} d\mathbf{z} - \int q(\mathbf{z}) \log q(\mathbf{z}) d\mathbf{z} \quad (28)$$

$$\leq \iint p_D(\mathbf{x}) q(\mathbf{z}|\mathbf{x}) \log q(\mathbf{z}|\mathbf{x}) d\mathbf{x} d\mathbf{z} - \int q(\mathbf{z}) \log p(\mathbf{z}) d\mathbf{z} \quad (29)$$

$$= \iint p_D(\mathbf{x}) q(\mathbf{z}|\mathbf{x}) \log q(\mathbf{z}|\mathbf{x}) d\mathbf{x} d\mathbf{z} - \iint p_D(\mathbf{x}) q(\mathbf{z}|\mathbf{x}) \log p(\mathbf{z}) d\mathbf{x} d\mathbf{z} \quad (30)$$

$$= \iint p_D(\mathbf{x}) q(\mathbf{z}|\mathbf{x}) \log \frac{q(\mathbf{z}|\mathbf{x})}{p(\mathbf{z})} d\mathbf{x} d\mathbf{z} \quad (31)$$

$$\equiv R^{\text{AVG}} \quad (32)$$

$$\implies I_q(\mathbf{X}; \mathbf{Z}) \leq R^{\text{AVG}} \quad (33)$$

where the inequality in (29) follows from (25).

The difference between the average KL and the mutual information is the aggregate KL:

$$R^{\text{AVG}} - I_q(\mathbf{X}; \mathbf{Z}) = \iint p_D(\mathbf{x}) q(\mathbf{z}|\mathbf{x}) \log \frac{q(\mathbf{z})}{p(\mathbf{z})} d\mathbf{x} d\mathbf{z} \quad (34)$$

$$= \int q(\mathbf{z}) \log \frac{q(\mathbf{z})}{p(\mathbf{z})} d\mathbf{z} \quad (35)$$

$$= D_{\text{KL}}(q(\mathbf{z}) \| p(\mathbf{z})) \quad (\text{Aggregate KL}) \quad (36)$$

C.2 Hierarchically bounding mutual information

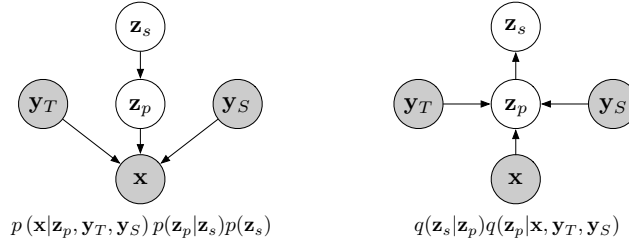


Figure C.1: Hierarchical decomposition of the latents. Shaded nodes indicate observed variables. [left] The true generative model. [right] Variational posterior that matches the form of the true posterior.

The model with hierarchical latents shown in Figure C.1 gives us the following:

$$p(\mathbf{z}) = p(\mathbf{z}_s, \mathbf{z}_p) = p(\mathbf{z}_p|\mathbf{z}_s) p(\mathbf{z}_s) \quad (37)$$

$$q(\mathbf{z}|\mathbf{x}) = q(\mathbf{z}_s, \mathbf{z}_p|\mathbf{x}) = q(\mathbf{z}_p|\mathbf{x}) q(\mathbf{z}_s|\mathbf{z}_p) \quad (38)$$

The conditional dependencies \mathbf{y}_T and \mathbf{y}_S are omitted for compactness.

Define marginal aggregated posteriors:

$$q(\mathbf{z}_p) \equiv \int p_D(\mathbf{x}) q(\mathbf{z}_p|\mathbf{x}) d\mathbf{x} \quad (39)$$

$$q(\mathbf{z}_s) \equiv \int q(\mathbf{z}_p) q(\mathbf{z}_s|\mathbf{z}_p) d\mathbf{z}_p \quad (40)$$

We can write the average joint KL term and mutual information as follows:

$$R^{\text{AVG}} = \int p_D(\mathbf{x}) [D_{\text{KL}}(q(\mathbf{z}_s|\mathbf{z}_p)q(\mathbf{z}_p|\mathbf{x}) \| p(\mathbf{z}_p|\mathbf{z}_s)p(\mathbf{z}_s))] d\mathbf{x} \quad (41)$$

$$I_q(\mathbf{X}; [\mathbf{Z}_s, \mathbf{Z}_p]) = \int p_D(\mathbf{x}) [D_{\text{KL}}(q(\mathbf{z}_s|\mathbf{z}_p)q(\mathbf{z}_p|\mathbf{x}) \| q(\mathbf{z}_s|\mathbf{z}_p)q(\mathbf{z}_p))] d\mathbf{x} \quad (42)$$

Next we show that $I_q(\mathbf{X}; [\mathbf{Z}_s, \mathbf{Z}_p]) = I_q(\mathbf{X}; \mathbf{Z}_p)$:

$$I_q(\mathbf{X}; [\mathbf{Z}_s, \mathbf{Z}_p]) = \iiint p_D(\mathbf{x}) q(\mathbf{z}_s, \mathbf{z}_p|\mathbf{x}) \log \frac{q(\mathbf{z}_s|\mathbf{z}_p)q(\mathbf{z}_p|\mathbf{x})}{q(\mathbf{z}_s|\mathbf{z}_p)q(\mathbf{z}_p)} d\mathbf{x} d\mathbf{z}_s d\mathbf{z}_p \quad (43)$$

$$= \iiint p_D(\mathbf{x}) q(\mathbf{z}_s, \mathbf{z}_p|\mathbf{x}) \log \frac{q(\mathbf{z}_p|\mathbf{x})}{q(\mathbf{z}_p)} d\mathbf{x} d\mathbf{z}_s d\mathbf{z}_p \quad (44)$$

$$= \iint p_D(\mathbf{x}) q(\mathbf{z}_p|\mathbf{x}) \log \frac{q(\mathbf{z}_p|\mathbf{x})}{q(\mathbf{z}_p)} d\mathbf{x} d\mathbf{z}_p \quad (45)$$

$$= I_q(\mathbf{X}; \mathbf{Z}_p) \quad (46)$$

Bound $I_q(\mathbf{X}; \mathbf{Z}_p)$:

$$I_q(\mathbf{X}; [\mathbf{Z}_s, \mathbf{Z}_p]) = I_q(\mathbf{X}; \mathbf{Z}_p) \quad (47)$$

$$I_q(\mathbf{X}; [\mathbf{Z}_s, \mathbf{Z}_p]) \leq R^{\text{AVG}} \quad (48)$$

$$\implies I_q(\mathbf{X}; \mathbf{Z}_p) \leq R^{\text{AVG}} \quad (49)$$

where (48) was shown in eq. (33).

Again, using the non-negativity of the KL, we can bound $I_q(\mathbf{Z}_s; \mathbf{Z}_p)$:

$$I_q(\mathbf{Z}_s; \mathbf{Z}_p) = \iint q(\mathbf{z}_s|\mathbf{z}_p)q(\mathbf{z}_p) \log \frac{q(\mathbf{z}_s|\mathbf{z}_p)}{q(\mathbf{z}_s)} d\mathbf{z}_s d\mathbf{z}_p \quad (50)$$

$$\leq \iint q(\mathbf{z}_s|\mathbf{z}_p)q(\mathbf{z}_p) \log \frac{q(\mathbf{z}_s|\mathbf{z}_p)}{p(\mathbf{z}_s)} d\mathbf{z}_s d\mathbf{z}_p \quad (51)$$

$$= \iiint p_D(\mathbf{x}) q(\mathbf{z}_s|\mathbf{z}_p)q(\mathbf{z}_p|\mathbf{x}) \log \frac{q(\mathbf{z}_s|\mathbf{z}_p)}{p(\mathbf{z}_s)} d\mathbf{z}_s d\mathbf{z}_p d\mathbf{x} \quad (52)$$

$$= \iint p_D(\mathbf{x}) q(\mathbf{z}_p|\mathbf{x}) D_{\text{KL}}(q(\mathbf{z}_s|\mathbf{z}_p) \| p(\mathbf{z}_s)) d\mathbf{z}_p d\mathbf{x} \quad (53)$$

$$\equiv R_s^{\text{AVG}} \quad (54)$$

$$I_q(\mathbf{X}; \mathbf{Z}_s) \leq I_q(\mathbf{Z}_p; \mathbf{Z}_s) \quad (55)$$

$$\implies I_q(\mathbf{X}; \mathbf{Z}_s) \leq R_s^{\text{AVG}} \quad (56)$$

where (55) can be demonstrated by applying the data processing inequality to a reversed version of the Markov chain, $\mathbf{X} \rightarrow \mathbf{Z}_p \rightarrow \mathbf{Z}_s$

Define R_p :

$$R_p \equiv R - R_s \quad (57)$$

$$= \iint q(\mathbf{z}_p|\mathbf{x})q(\mathbf{z}_s|\mathbf{z}_p) \log \frac{q(\mathbf{z}_p|\mathbf{x})}{p(\mathbf{z}_p|\mathbf{z}_s)} d\mathbf{z}_s d\mathbf{z}_p \quad (58)$$

Giving us the following bounds on $I_q(\mathbf{X}; \mathbf{Z}_p)$ and $I_q(\mathbf{X}; \mathbf{Z}_s)$:

$$\implies I_q(\mathbf{X}; \mathbf{Z}_s) \leq R_s^{\text{AVG}}, \quad I_q(\mathbf{X}; \mathbf{Z}_p) \leq R_s^{\text{AVG}} + R_p^{\text{AVG}} \quad (59)$$